

DEVELOPMENT OF NILOTINIB LOADED SOLID LIPID NANOPARTICLES AND OPTIMIZATION BY CENTRAL COMPOSITE DESIGN APPROACH

JARPULA ARUN KUMAR¹, D. V. R. N. BHIKSHAPATHI^{2*}

^{1,2}Career Point University, Kota, Rajasthan 325003, India

Email: dbpathi71@gmail.com

Received: 20 Dec 2021, Revised and Accepted: 28 Jan 2022

ABSTRACT

Objective: In current research, solid lipid nanoparticles (SLN) are formulated for the anticancer drug, nilotinib, to conquer the drawbacks associated with drug including low bioavailability and solubility.

Methods: The formulation comprised of tripalmitin (lipid), poloxamer 188 (surfactant) and glyceryl palmitostearate (cosurfactant) by solvent evaporation technique. The formulation and process variables of SLN were optimized by experimental design-Central composite design (CCD). The effect of drug to lipid ratio (A), concentration of Poloxamer 188 (B) and concentration of glyceryl palmitostearate (C), on particle size (Y1) and encapsulation efficiency (Y2) of SLN were evaluated. Three batches (F1-F3) of Nilotinib SLNs were formulated by desirability approach and evaluated.

Results: The mean size of all the formulations ranged between 187–198 nm, PDI between 0.291–0.652 and zeta potential between -21.8 to -24.7 mV indicating the wide range of size distribution and stability of the formulations. The total encapsulation efficiency of SLNs ranged between 85 to 86 %. The SEM analysis revealed the spherical shape of individual particles and PXRD results indicate amorphization of drug in SLN formulation. The drug release was continued for 24 h, indicative of controlled release drug delivery.

Conclusion: From the above results it is concluded that the solubility and bioavailability of nilotinib is enhanced.

Keywords: Solid Lipid Nanoparticles (SLN), Nilotinib, Leukemia, Central composite design (CCD)

© 2022 The Authors. Published by Innovare Academic Sciences Pvt Ltd. This is an open access article under the CC BY license (<https://creativecommons.org/licenses/by/4.0/>) DOI: <https://dx.doi.org/10.22159/ijap.2022v14i2.43943>. Journal homepage: <https://innovareacademics.in/journals/index.php/ijap>

INTRODUCTION

The drug nilotinib is second-generation kinase inhibitor for chronic inflammatory diseases Leukemia, caused by the breakpoint cluster region of Abelson murine leukemia (BCR-ABL) gene. It inhibits tyrosine kinase activity of the BCR-ABL protein [1]. However, the deprived solubility of drug results in lower oral absorption [2, 3]. Nilotinib's solubility limits its therapeutic efficacy partly, due to the limited exposure it gives to the drug.

Increasing interest in lipid-based pharmaceutical delivery systems has come about because they have increased bioavailability [4]. Lipid-based formulations have emerged as an effective and versatile technology for many class IV BCS drugs [5, 6]. As an alternative to emulsions, SLNs contain solid lipids instead of liquid oils.

Solid lipid nanoparticles (SLN) are colloidal particles of 50–1000 nm size range comprising of lipid components that are solids dispersed in aqueous surfactant aided by an emulsifier. The SLN formulations are more biocompatible and don't leave any organic solvent residues. They also offer the viability of scale-up, hydrophilic and hydrophobic drug encapsulation and surface conjugation [7-11]. However, SLNs suffer lower drug loading, impulsive drug dissolution, and the risk of gelation due to polymorphism [12].

It was necessary to employ a statistical experiment design methodology in order to optimize the formulation and process variables of the SLNs. CCD is the best strategy to allocate each variable to a range of evaluations while obtaining a consistent curvature judgment to attain rational information to test for "lack-of-fit" by rationalized number of design points [13, 14]. After selecting the critical variables affecting particle size (PLS), encapsulation efficiency (ENE), the response surface methodology (RSM), followed by CCD were employed to optimize these variable levels. The study is novel in that it successfully prepared and characterized a non-lipidic, temperature degradable low soluble nilotinib anti-cancer drug into an SLN carrier newly using central composite design for optimization, as well as shown enhanced solubility of the same.

MATERIALS AND METHODS

Materials

Nilotinib was obtained as a gift sample from Dr. Reddy's laboratories Limited, Hyderabad, India. (Trimyristin (Dynasan-114), tripalmitin (Dynasan-116) and tristearin (Dynasan-118), Sodium taurocholate, and glyceryl palmitostearate purchased from Sigma Aldrich (USA). Poloxamer-188 gifted by Dr. Reddy's lab Ltd., India.

Solubility study by equilibrium solubility method

We conducted solubility studies using 200 mg of the drug per ml in 25 ml of conical flasks, 15 ml of various solvents, and several hours of vortexing under rotatory shakers. After filtering and dilution, UV spectrophotometer at 263 nm was used to read the absorbance values. Distilled water, ethanol, methanol, benzene, dimethylsulfoxide, dimethylformamide, propylene glycol, pH 1.2, 5.5, 6.8 and 7.4 phosphate buffers were evaluated. Three independent studies were conducted [15].

Development of SLN formulation

Preliminary experiments

Several formulation parameters and process variables were optimized to achieve the desired PLS, polydispersity index, zeta potential, and ENE. We prepared formulations by changing one parameter at a time while maintaining other parameters constant.

Selection of formulation excipients

Preliminary experiment was carried out with three different lipids (Dynasan-114/116/118) and surfactants (Tween80, Poloxamer188 and polyvinylalcohol) followed by evaluation. Selection of co-surfactants was performed by the titration method [16].

Optimization of process variables

We carried out preliminary optimization of homogenization speed and time, sonication time, and stirring speed and time by conducting the experiment at four different RPMs (4,000 to 8,000), for different

times (2, 4, 6 and 8 min) at room temperature, in order to achieve a coarse emulsion [17].

The obtained emulsion was then sonicated for a variety of periods of time (5-20 min) to obtain a nanoemulsion. The formulation was evaporated to dryness. For optimization, the formulation was stirred at various speeds (500, 1000, and 1500 rpm), and for times (1, 2 and 3 h).

Design of experiments

Based on results from preliminary studies, we establish that the ratio of drug to lipid (A), the conc. of poloxamer 188 (B) and the conc. of glyceryl palmitostearate (C) had significant impacts on the PLS (Y1) and ENE (Y2) of SLNs [18].

The range of levels of these variables was resolute based on preliminary experimental results and is shown in table 1. Based upon the CCD presented by Stat-Ease Design Expert® software V8.0.1, 20 model experimental runs were systematically arranged. Homogenization speed (8000 rpm), homogenization time (6 min), sonication time (10 min), stirring speed (1000 rpm) and stirring time (3 h) were kept constant throughout all the experiments. Table 2 presents the experimental conditions for all model experiments.

Measurement of responses

The PLS of the prepared formulation was evaluated using Malvern PLS analyzer (Master sizer 2000, Malvern, UK) [19].

About 10 ml of SLN centrifuged at 10,000 rpm, 20 min at 25 °C (Remi InstPvt. Ltd, India) followed by isolation of lipid portion and evaluated at spectrophotometrically at λmax263 nm (Shimadzu 1800, Japan). The %ENE calculated as follows

$$EE(\%) = \frac{\text{Totaldrug(mg)} - \text{Freedrug(mg)}}{\text{Total drug(mg)}} \times 100$$

Data analysis

Linear, quadratic and cubic models can be used to describe the relationship between dependent and independent variables.

Numerous statistical parameters, comprising the p-value of the model, p-value of lack of fit, multiple regression coefficients (R²), adjusted multiple regression coefficients (adjusted R²), coefficient of variation was considered to select a suitable fitting model. The terms with p-value greater than 0.0005 were considered as insignificant and were eliminated from the model. Each response parameter was evaluated by quadratic model using multiple regression analysis as shown in the equation.

$$Y = A_0 + A_1 X_1 + A_2 X_2 + A_3 X_3 + A_{11} X_1^2 + A_{22} X_2^2 + A_{33} X_3^2 + A_{12} X_1 X_2 + A_{13} X_1 X_3 + A_{23} X_2 X_3$$

Where Y-Response parameter

A₀-Intercept

A₁, A₂, A₃-linear regression coefficients

A₁₁, A₂₂, A₃₃-quadratic regression coefficients

A₁₂, A₂₃, A₁₃-interaction regression coefficients

X₁, X₂ and X₃-Main influencing factors

X₁X₂-Interactive effect

X₁², X₂²and X₃²-Quadratic effect

The independent variables (IDV) which do not contribute to the regression equation will be deleted one at a time by the backward elimination procedure. Three-dimensional response surface plots (RSP) show the functional relation among a selected dependent variable (DV) and two IDV. The perturbation (PBP) and contour plots (CP) also can be used to visualize the effect of independent variables on the response parameters [20, 21].

Optimization and confirmation experiments

Setting restraints on DV and IDV led to the creation of an optimized composition. The statistical experimental strategy was verified by three additional confirmation experiments.

Table 1: CCD design

IDV		Levels				
Variable	Name	Units	-1	+1	-α	+α
A	Drug to lipid ratio	-	0.1	0.3	0.07	0.33
B	Concentration of poloxamer 188	mg	40	80	33.68	86.32
C	Concentration of glyceryl palmitostearate	mg	20	40	16.84	43.16
DV		Goal				
Y1	PLS	nm	Minimize			
Y2	ENE	%	Maximize			

Table 2: CCD with observed response

Run	Drug to lipid ratio (A)	Conc. of poloxamer 188 (B)	Conc. of Glyceryl palmitostearate (C)	Particle size (Y1)	Encapsulation efficiency (Y2)
1	0.2	86.32148	30	121.54	81.22
2	0.2	60	30	102.56	78.34
3	0.1	80	40	428.56	96.72
4	0.331607	60	30	96.72	64.78
5	0.3	40	40	80.98	67.89
6	0.3	80	20	76.87	68.34
7	0.3	80	40	74.82	69.72
8	0.2	60	30	103.12	77.98
9	0.3	40	20	82.43	66.12
10	0.068393	60	30	592.12	99.34
11	0.2	33.67852	30	145.92	75.68
12	0.2	60	30	102.12	78.96
13	0.2	60	43.16074	106.72	80.12
14	0.2	60	30	102.21	78.34
15	0.1	80	20	449.86	95.12
16	0.2	60	30	102.89	78.86
17	0.2	60	30	102.39	78.12
18	0.1	40	20	481.84	93.12
19	0.1	40	40	460.48	94.72
20	0.2	60	16.83926	121.72	77.12

Preparation of nilotinib loaded SLN

The SLNs were prepared by emulsification combined with the solvent evaporation technique [22]. In order to isolate nilotinib (200 mg), Trimyrustin (Dynasan-114), and glyceryl palmitostearate, three ml of chloroform were dissolved in 10 ml of 1.5% w/v poloxamer 188 solution. In order to homogenize the dispersion, it was homogenized at 8000 rpm for eight minutes and sonicated for ten minutes. Mixture was stirred at 1000 revolutions per minute for 3 h. An emulsion of nanoparticles has been centrifuged at 12000 revolutions per minute for 45 min. The SLNs were washed with milliQ water and cryoprotected with trehalose-dihydrate.

Characterization of SLN

The PLS, polydispersity index (PDI) and zeta potential (ZP) of the SLNs were measured by using a Zetasizer (Nano ZS90, Malvern, Worcestershire, UK).

The ENE values evaluated as per the procedure mentioned earlier

The % drug loading was calculated as.

$$DL(\%) = \frac{\text{Loaded drug (mg)}}{\text{Total lipid in the formulation (mg)}} \times 100$$

The scanning electron microscopy (SEM) and powder X-ray diffractometry (PXRD) studies

The Scanning Electron Microscope (SEM, Hitachi, Tokyo, Japan) was used to record the image of suitably diluted samples. The PXRD was recorded using Powder X-ray diffractometer (Multiflex, M/s. Rigaku, Tokyo, Japan) as per the referred procedure [23].

In vitro dissolution

The study conducted in USP apparatus II was used for 48 h. The SLN suspension was diluted using simulated intestinal fluid (SIF, pH 6.7) in 1: 9 ratio and stirred at 37 °C at a speed of 50 rpm. After a

predetermined period of time, 2 ml of the dissolution medium was withdrawn, ultra-filtered as described above, and its absorption was measured at 263 nm by UV absorption. In its place, a second SIF (37 °C) at the same volume was added [24].

Drug release kinetics

The results of drug release were fitted into various kinetic models, Data obtained from *in vitro* release studies were fitted to various kinetic equations [25].

Stability studies

Nilotinib SLNs suspended in screw-capped glass vials were analyzed for stability over 60 d. Each group of six samples was stored at 25 °C and 4 °C. A number of measurements were made with regard to drug leakage from nanoparticles and mean particle sizes of samples after 1, 7, 15, 30, 45, and 60 d [26].

Data analysis

Data are expressed as the mean±standard deviation (SD) of the mean and statistical analysis was carried out employing the one-way analysis of variance (ANOVA). A value of p<0.05 was considered statistically significant.

RESULTS

Optimization of process variables

The formulation was stirred at different speed (500, 1000 and 1500 rpm) and for different time period (1, 2, and 4 h) for optimization.

Twenty experiments were carried out based on the CCD (table 2). The results indicate that the dependent variables are sturdily dependent on chosen independent variables, as shown in all 20 batches.

The summary of the design is as shown in fig. 1.

File Version	8.0.1.0	
Study Type	Response Surface	Runs 20
Design Type	Central Composite	Blocks No Blocks
Design Model	Quadratic	Build Time (ms) 3.44

Factor	Name	Units	Type	Subtype	Minimum	Maximum	-1 Actual	+1 Actual	Mean	Std. Dev
A	Drug to lipid ratio		Numeric	Continuous	0.07	0.33	0.10	0.30	0.20	0.08
B	Concentration of poloxamer	mg	Numeric	Continuous	33.68	86.32	40.00	80.00	60.00	15.14
C	concentration of glyceryl pal	mg	Numeric	Continuous	16.84	43.16	20.00	40.00	30.00	7.57

Response	Name	Units	Obs	Analysis	Minimum	Maximum	Mean	Std. Dev.	Ratio	Trans	Model
Y1	Particle size	nm	20	Polynomial	74.82	592.12	196.793	172.578	7.91393	None	RQuadratic
Y2	encapsulation efficiency	%	20	Polynomial	64.78	99.34	80.0305	10.5819	1.5335	None	RQuadratic

Fig. 1: Summary of the central composite design

Table 3: Regression equation for-Y1 and Y2

Response	Equation
Y1	102.54-188.2 A-9.39 B-5.74 C+6.52 AB+4.89 AC+139.55 A ² +18.01 B ² +6.75 C ²
Y2	78.4-13.35 A+1.33 B+0.89 C+2.41 A ² +0.42 C ²

According to table 2, the PLS ranged between 74.2-592.12 nm. In the statistical analysis generated for PLS (Y1), it was determined that the model is significant with an F-value of 810324 (table 3). Using the PBP, 3D RSP and CP plots the main and interactive effects of IDV are revealed. A has the largest impact on Y1 followed by B and C, which have a moderate effect. As the ratio of drug to lipid decreases, the wavelength of

Y1 augments from 428.56 nm to 481.84 nm. A high level of A results in Y1 increasing from 74.82 nm to 82.43 nm. As the amount of B decreases, Y1 decreases from 481.84 nm to 80.98 nm. In the same way, at high level of B, Y1 decreases from 449.86 nm to 74.8 when levels of C are low, Y1 decreases from 481.84 nm to 76.87 nm. As well, at high level of C, Y1 decreases from 460.48 nm to 74.82 nm.

ENE of SLN was found to be in the range of 64.78–99.34 % (table 2). The equation results showcase that A has -ve effect and B and C have +ve effect on ENE. At lower A values, Y2 decreased from 96.72 %-93.12 %. At higher level of A, Y2 decreased from 69.72 %-66.12 %. At the lower level of B, Y2 augmented from 66.12 % to 94.72%. Similarly, at higher level of B, Y2 augmented from 68.34 % to 96.72 %. At low levels of C, Y2 augmented from 66.12 % to 95.12%. Similarly, at higher level of C, Y2 increased from 76.78% to 96.72%.

Design-Expert® Software
 Particle size
 Actual Factors
 A: Drug to lipid ratio = 0.20
 B: Concentration of poloxamer = 60.00
 C: concentration of glyceryl palmitostearate = 30.00

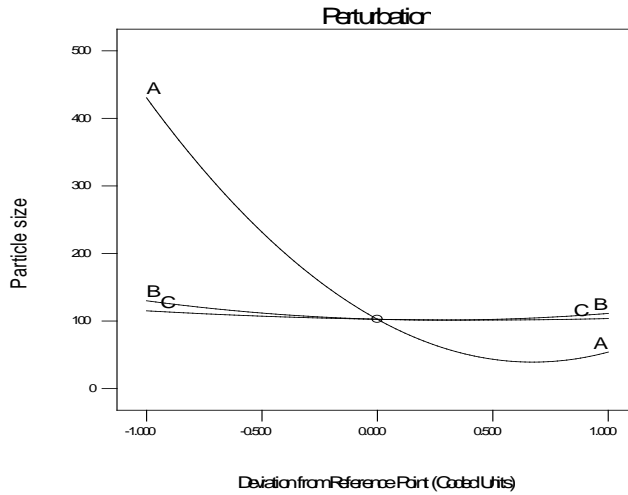
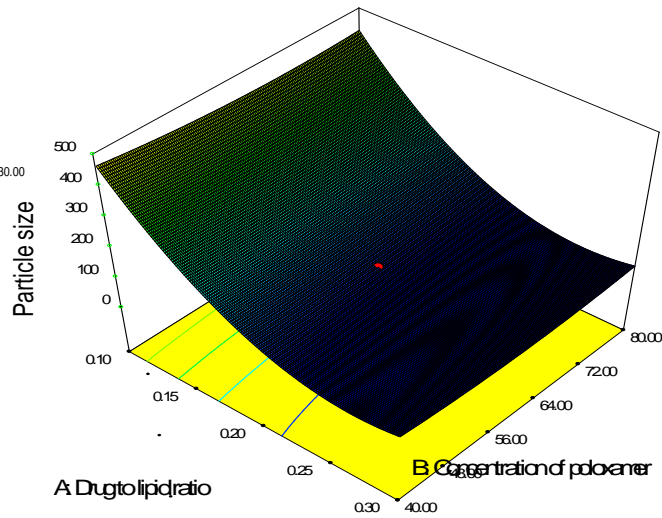


Fig. 2A: Perturbation plot showing the effect of A, B and C on particle size

B

Design-Expert® Software
 Particle size
 ● Design points above predicted value
 ○ Design points below predicted value
 592.12
 74.82
 X1 = A: Drug to lipid ratio
 X2 = B: Concentration of poloxamer
 Actual Factor
 C: concentration of glyceryl palmitostearate = 30.00



C

Design-Expert® Software
 Particle size
 ● Design Points
 592.12
 74.82
 X1 = A: Drug to lipid ratio
 X2 = B: Concentration of poloxamer
 Actual Factor
 C: concentration of glyceryl palmitostearate = 30.00

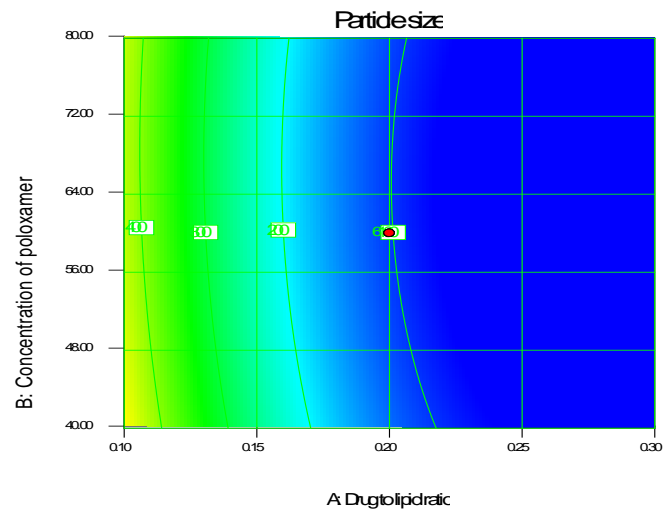
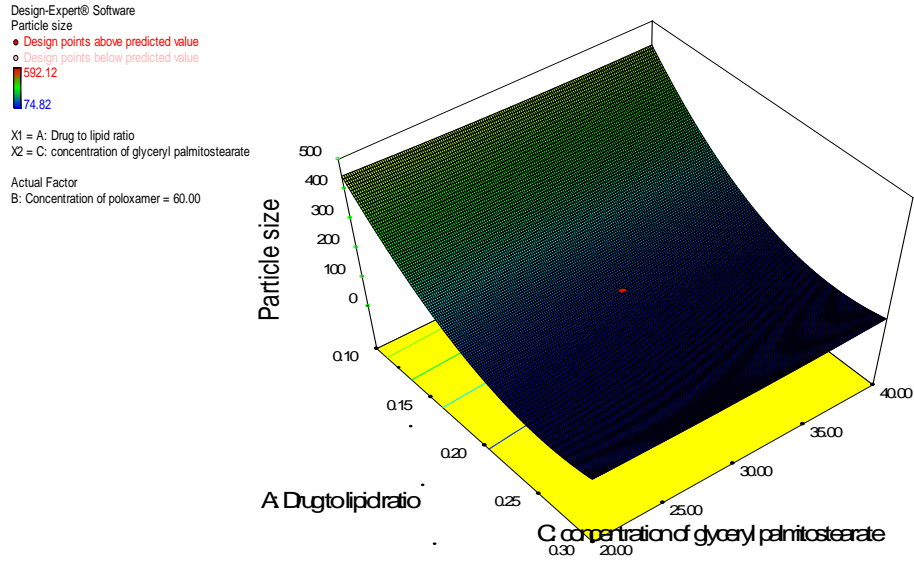


Fig. 2B: Response surface plot showing the interactive effect of A and B, at constant level of C 2C. Contour plot showing the interactive effect of A and B, at constant level of C

D



E

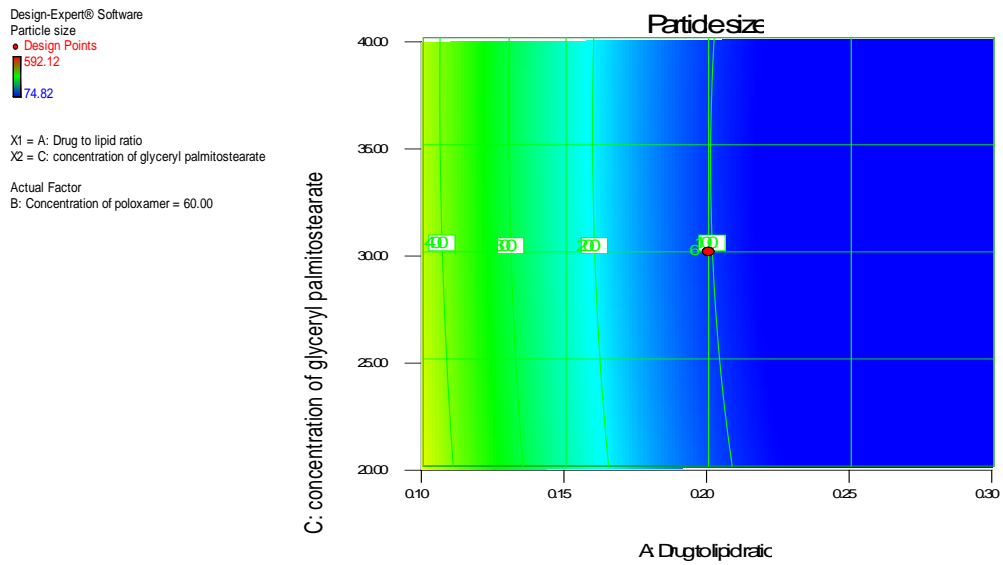


Fig. 2D: Response surface plot showing the interactive effect of A and C, at constant level of B 2E. Contour plot showing the interactive effect of A and C, at a constant level of B

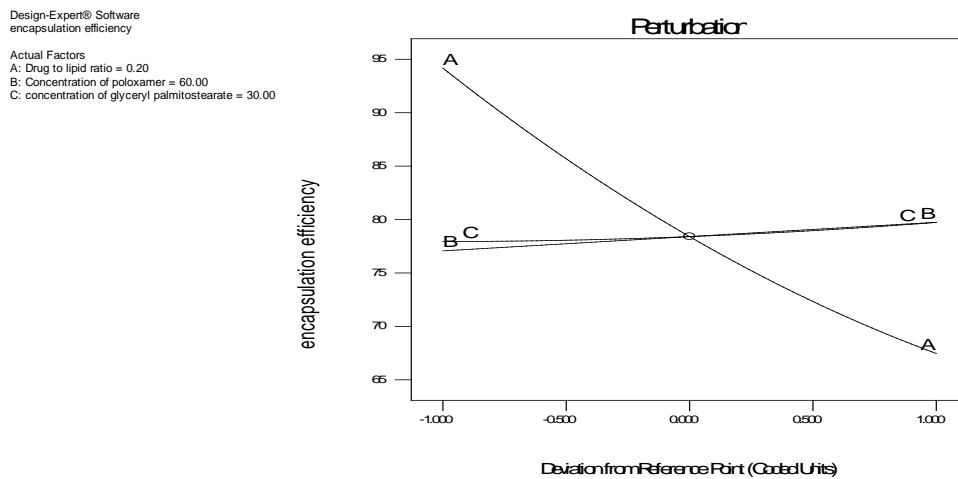


Fig. 3A: Perturbation plot showing the effect of A, B and C on % encapsulation efficiency

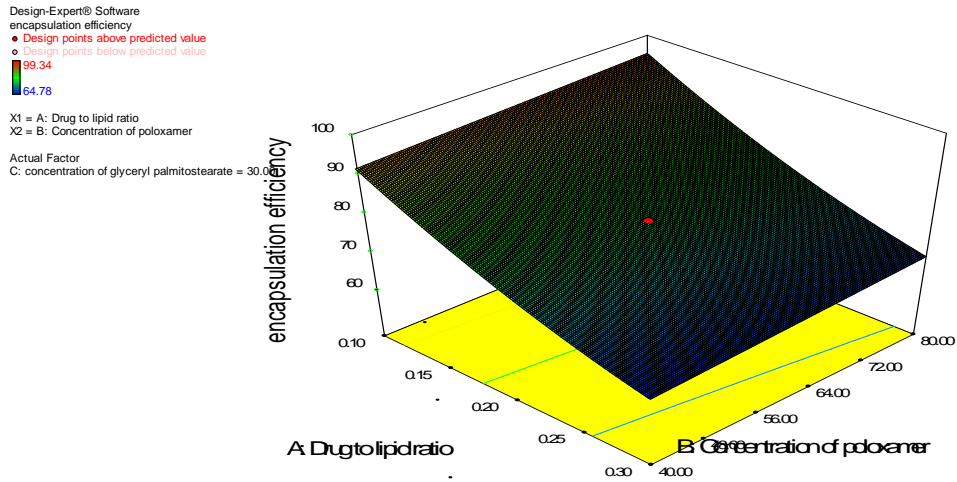


Fig. 3B: 3D-Response surface plot showing the influence A and B on encapsulation efficiency at constant level of C

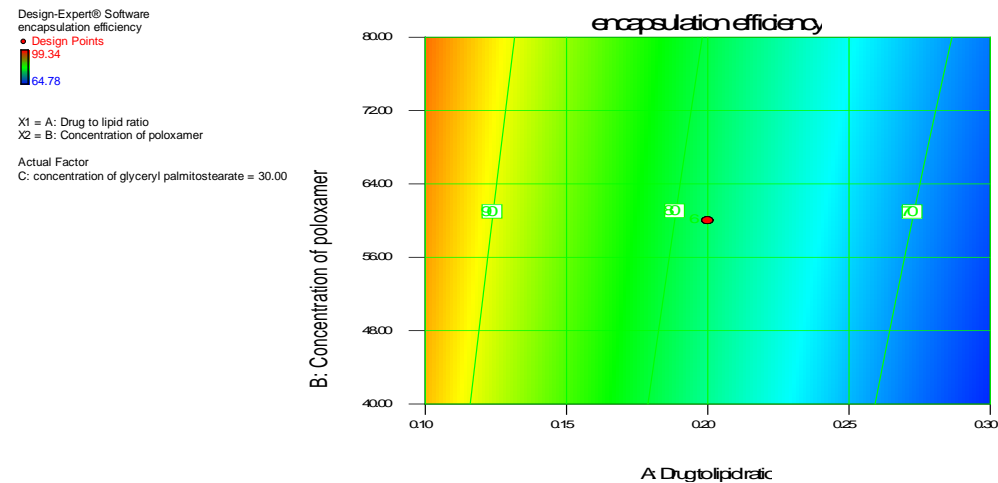


Fig. 3C: Contour plot showing the influence A and B on encapsulation efficiency at a constant level of C

Optimization and confirmation experiments

A numerical optimization method adopted with constraints like minimizing the PLS and to maximizing the ENE. Using the optimum settings, the SLNs with a desirability value of 0.691 was obtained. (table 4). For verification, 3 batches of SLNs were formulated in accordance with the predicted levels of A, B and C. Obtained Y1, and Y2 values were in good agreement with those

of predicted. The results demonstrate the reliability of the optimization technique.

The PLS of all the formulations ranged between 187.78±8.84 nm to 198.34±11.26 nm (table 5), while the PDI ranged between 0.291 to 0.652, indicating a wider of size distribution. The ZP of SLNs was between -21.8±1.58 mV to -24.7±1.22 mV indicating the stability of colloidal systems [27].

Table 4: Optimized values

Independent variable	Nominal values	Predicted		Observed*		
		(Y1)	(Y2)	Batch	(Y1)	(Y2)
Drug lipid ratio (A)	0.16	195.456	86.27	F1	198.34±11.26	86.18±2.12
Conc. of poloxamer 188 (B)	80			F2	187.78±8.84	85.78±1.39
Conc. of glyceryl palmitostearate (C)	40			F3	192.34±5.57	85.12±3.12

*(All determinations were performed in triplicate and values were expressed as mean±SD, n=3) (p<0.05)

Table 5: The PLS, PDI, ZP and ENE of SLN formulations

Batch	PLS±SD (nm)	PDI	ZP±SD (mV)	% EE±SD
F1	198.34±11.26	0.321	-23.7±2.34	86.18±2.12
F2	187.78±8.84	0.412	-21.8±1.58	85.78±1.39
F3	192.34±5.57	0.296	-24.7±1.22	85.12±3.12

(All determinations were performed in triplicate and values were expressed as mean±SD, n=3)(p<0.05)

SEM analysis

SEM analysis revealed the spherical shape of individual particles. The images in fig. 4 confirmed the nano size of the particles. SEM results were also in concurrence with PLS measurements.

PXRD pattern

X-ray diffraction of pattern of nilotinib has shown characteristic crystalline peaks, whereas in the formulation, the characteristic peaks of drug have been disappeared. The disappearance of characteristic peaks of the drug indicating the amorphization of drug [28]. (fig. 5).

Fig. 6 shows the *in vitro* release profile of nilotinib from nano formulation in SIF (pH 6.8). The amount of drug released from nano formulation was significantly higher than that from the nilotinib suspension. This was due to the fact that Nilotinib was hydrophobic

in nature and its solubility increases with nanoparticles, which resulted in the faster and enhanced release of Nilotinib from nanoparticles. The drug release profile from different formulations is presented in table 5. The drug release was continued for 24 h, indicative of controlled release drug delivery.

Release kinetics

Drug release data for the optimized formulation was fitted into various kinetic equations to find out the order and mechanism of drug release. The drug release followed the first-order kinetics ($R^2=0.96564$).

Stability study

Tables 6 do not indicate any considerable variation ($p<0.05$) in ENE and PLS of optimized SLN stored at refrigerated conditions and at room temperature [29, 30].

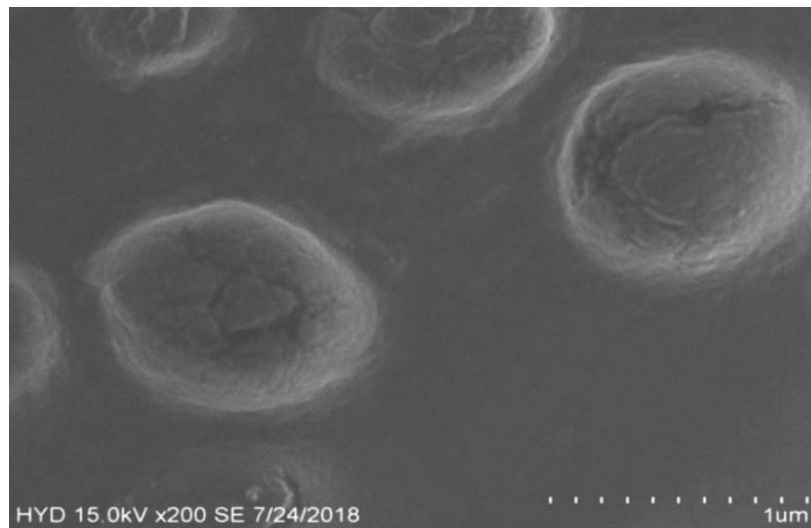


Fig. 4: SEM image of Nilotinib nanoparticles

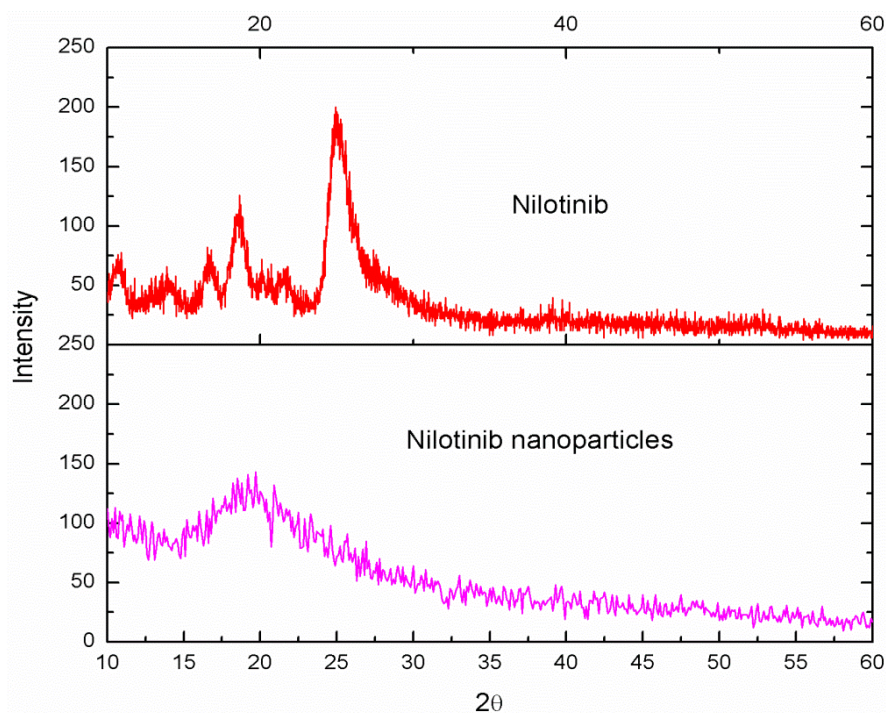


Fig. 5: X-ray diffraction pattern

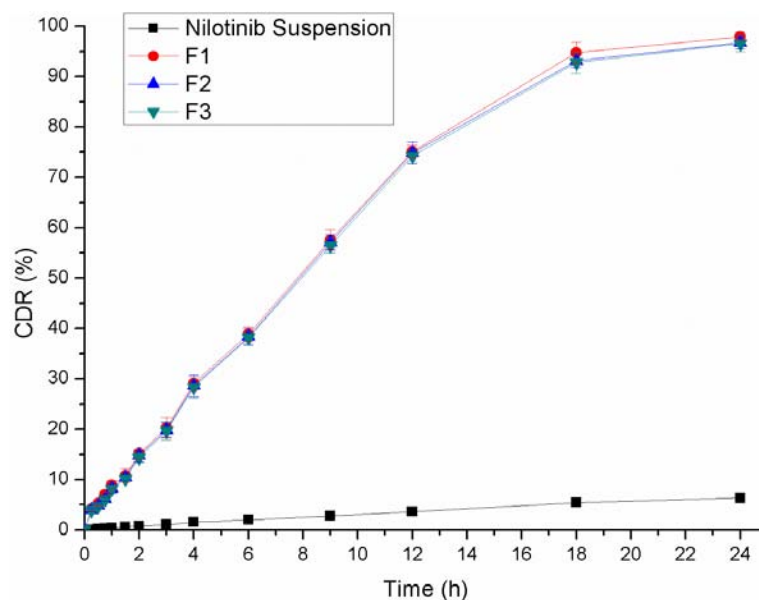


Fig. 6: Dissolution profile of nilotinib, (All determinations were performed in triplicate and values were expressed as mean \pm SD, n=3)

Table 6: PLS and ENE of nilotinib nanoparticles stability data

Temperature ($^{\circ}$ C)	PLS (nm)		ENE (%)		Release data (% CDR)			
	0 mo	3 mo	0 mo	3 mo	0 mo	3 mo	3 mo	3 mo
					30 min	1 h	30 min	1 h
4 \pm 1 $^{\circ}$ C	198.34 \pm 11.26	132.12 \pm 7.13	86.18 \pm 2.12	79.892 \pm 1.13	5.22 \pm 0.34	8.88 \pm 0.86	4.98 \pm 1.18	8.74 \pm 2.16
25 \pm 2 $^{\circ}$ C	198.34 \pm 11.26	138.16 \pm 9.12	86.18 \pm 2.12	77.142 \pm 0.68	5.22 \pm 0.34	8.88 \pm 0.86	8.12 \pm 0.86	12.28 \pm 4.52

(All determinations were performed in triplicate and values were expressed as mean \pm SD, n=3) (p<0.05).

CONCLUSION

This study demonstrates the application of a 3³ CCD and regression analysis for optimization of formulation variables in the preparation of Nilotinib SLNs. The optimized SLNs possess an imperfect crystalline lattice and a sphere-shaped. Significant augmentation in dissolution rate was observed. This study suggests that the developed Nilotinib SLN could execute therapeutically enhanced effects than the conventional formulations.

FUNDING

Nil

AUTHORS CONTRIBUTIONS

All the authors have contributed equally.

CONFLICT OF INTERESTS

Declared none

REFERENCES

- Bhamidipati PK, Kantarjian H, Cortes J, Cornelison AM, Jabbour E. Management of imatinib-resistant patients with chronic myeloid leukemia. *Ther Adv Hematol*. 2013;4(2):103-17. doi: 10.1177/2040620712468289, PMID 23610618.
- Xia B, Heimbach T, He H, Lin TH. Nilotinib preclinical pharmacokinetics and practical application toward clinical projections of oral absorption and systemic availability. *Biopharm Drug Dispos*. 2012;33(9):536-49. doi: 10.1002/bdd.1821, PMID 23097199.
- Tanaka MF, Kantarjian H, Cortes J, Ohanian M, Jabbour E. Treatment options for chronic myeloid leukemia. *Expert Opin Pharmacother*. 2012 Apr 1;13(6):815-28. doi: 10.1517/14656566.2012.671296, PMID 22429140.
- Rane SS, Anderson BD. What determines drug solubility in lipid vehicles: is it predictable? *Adv Drug Deliv Rev*. 2008 Mar 17;60(6):638-56. doi: 10.1016/j.addr.2007.10.015, PMID 18089295.
- Markovic M, Ben-Shabat S, Aponick A, Zimmermann EM, Dahan A. Lipids and lipid-processing pathways in drug delivery and therapeutics. *Int J Mol Sci*. 2020 Jan;21(9):3248. doi: 10.3390/ijms21093248, PMID 32375338.
- Chakraborty S, Shukla D, Mishra B, Singh S. Lipid-an emerging platform for oral delivery of drugs with poor bioavailability. *Eur J Pharm Biopharm*. 2009 Sep 1;73(1):1-15. doi: 10.1016/j.ejpb.2009.06.001, PMID 19505572.
- Mehnert W, Mäder K. Solid lipid nanoparticles: production, characterization and applications. *Adv Drug Deliv Rev*. 2001;47(2-3):165-96. doi: 10.1016/S0169-409X(01)00105-3. PMID 11311991.
- Bargoni A, Cavalli R, Zara GP, Fundarò A, Caputo O, Gasco MR. Transmucosal transport of tobramycin incorporated in solid lipid nanoparticles (SLN) after duodenal administration to rats. Part II—tissue distribution. *Pharmacol Res*. 2001 May 1;43(5):497-502. doi: 10.1006/phrs.2001.0813, PMID 11394943.
- Cavalli R, Bargoni A, Podio V, Muntoni E, Zara GP, Gasco MR. Duodenal administration of solid lipid nanoparticles loaded with different percentages of tobramycin. *J Pharm Sci*. 2003 May 1;92(5):1085-94. doi: 10.1002/jps.10368, PMID 12712429.
- De Rossi ED, Ainsa JA, Riccardi G. Role of mycobacterial efflux transporters in drug resistance: an unresolved question. *FEMS Microbiol Rev*. 2006 Jan 1;30(1):36-52. doi: 10.1111/j.1574-6976.2005.00002.x, PMID 16438679.
- Dingler A, Gohla S. Production of solid lipid nanoparticles (SLN): scaling up feasibilities. *J Microencapsul*. 2002 Jan 1;19(1):11-6. doi: 10.1080/02652040010018056, PMID 11811752.
- Hu FQ, Jiang SP, Du YZ, Yuan H, Ye YQ, Zeng S. Preparation and characteristics of monostearin nanostructured lipid carriers. *Int J Pharm*. 2006 May 11;314(1):83-9. doi: 10.1016/j.ijpharm.2006.01.040, PMID 16563671.

13. Nagar M, Panwar KS, Chopra VS, Bala I, Trivedi P. Quality by design: A systematic approach to pharmaceutical development. *Pharm Lett.* 2010;2(2):111-30.
14. Kakodkar S, Sharmada S. Pharmaceutical quality-by-design (QbD): basic principles. *Int J Res Methodol.* 2015;1(1).
15. Pouton CW, Porter CJ. Formulation of lipid-based delivery systems for oral administration: materials, methods and strategies. *Adv Drug Deliv Rev.* 2008 Mar 17;60(6):625-37. doi: 10.1016/j.addr.2007.10.010, PMID 18068260.
16. Wissing SA, Kayser O, Muller RH. Solid lipid nanoparticles for parenteral drug delivery. *Adv Drug Deliv Rev.* 2004;56(9):1257-72. doi: 10.1016/j.addr.2003.12.002, PMID 15109768.
17. Mehnert W, Mader K. Solid lipid nanoparticles: production, characterization and applications. *Adv Drug Deliv Rev.* 2001;47(2-3):165-96. doi: 10.1016/s0169-409x(01)00105-3, PMID 11311991.
18. Myers RH, Montgomery DC, Anderson Cook CM. Response surface methodology, product and process optimization using experimental design. 4th ed. Wiley; 2016.
19. Grana A, Limpach A, Chauhan H. Formulation considerations and applications of solid lipid nanoparticles. *Am Pharm Rev.* 2013;16(1):19-25.
20. Shivakumar HN, Patel PB, Desai BG, Ashok P, Arulmozhi S. Design and statistical optimization of glipizide loaded lipospheres using response surface methodology. *Acta Pharm.* 2007;57(3):269-85. doi: 10.2478/v10007-007-0022-8, PMID 17878108.
21. Nazzal S, Khan MA. Response surface methodology for the optimization of ubiquinone self-nano emulsified drug delivery system. *AAPS PharmSciTech.* 2002;3(1):E3. doi: 10.1208/pt030103, PMID 12916956.
22. Pooja D, Kulhari H, Tunki L, Chinde S, Kuncha M, Grover P, Rachamalla SS, Sistla R. Nanomedicines for targeted delivery of etoposide to non-small cell lung cancer using transferrin functionalized nanoparticles. *RSC Adv.* 2015;5(61):49122-31. doi: 10.1039/C5RA03316K.
23. Barman RK, Iwao Y, Funakoshi Y, Ranneh AH, Noguchi S, Wahed MI, Itai S. Development of highly stable nifedipine solid-lipid nanoparticles. *Chem Pharm Bull (Tokyo).* 2014;62(5):399-406. doi: 10.1248/cpb.c13-00684, PMID 24789922.
24. Shen J, Burgess DJ. *In vitro* dissolution testing strategies for nanoparticulate drug delivery systems: recent developments and challenges. *Drug Deliv Transl Res.* 2013;3(5):409-15. doi: 10.1007/s13346-013-0129-z, PMID 24069580.
25. Costa P, Sousa Lobo JM. Modeling and comparison of dissolution profiles. *Eur J Pharm Sci.* 2001 May 1;13(2):123-33. doi: 10.1016/s0928-0987(01)00095-1, PMID 11297896.
26. Freitas C, Muller RH. Correlation between long-term stability of solid lipid nanoparticles (SLN) and crystallinity of the lipid phase. *Eur J Pharm Biopharm.* 1999 Mar;47(2):125-32. doi: 10.1016/s0939-6411(98)00074-5, PMID 10234536.
27. Begum MY, Gudipati PR. Formulation and evaluation of dasatinib-loaded solid lipid nanoparticles. *Int J Pharm Pharm Sci.* 2018;10(12):14. doi: 10.22159/ijpps.2018v10i12.27567.
28. Taraka Sunil Kumar K, Mohan Varma M, Ravi Prakash. Development and optimization of enzalutamide-loaded solid lipid nanoparticles using box-behnken design. *Asian J Pharm Clin Res.* 2019;12:67-76.
29. Sawant P, Karekar P, Waghmare K. Formulation and characterization of solid lipid nanoparticles containing ginger oil for enhancement of stability. *Int J Pharm Pharm Sci.* 2020 Jun;12(6):36-44. doi: 10.22159/ijpps.2020v12i6.37357.
30. Manoj, Padhi, Sasmita. Solid lipid nanoparticles—a review. Article, review and sarangi. *Crit Rev.* 2016;3:5-12.